

ESTIMATION OF ANISOTROPY PARAMETERS WITH THE i-CRS OPERATOR

C. Vanelle, K. Sager, B. Schwarz, B. Kashtan, and D. Gajewski

email: *claudia.vanelle@zmaw.de*

keywords: *parameter determination, anisotropy, multiparameter, CRS*

ABSTRACT

Traveltime operators are a foundation of seismic data processing and imaging. A large number of such expressions exists for the description of traveltime surfaces, beginning with the classical NMO formula to multiparameter stacking operators like the common reflection surface (CRS) or multifocusing. Application of these operators leads to simulated zero-offset sections with improved signal-to-noise ratio and parameter sets that can be related to an underlying earth model. In particular, multiparameter operators for isotropic media can handle curved subsurface structures. The accuracy often depends on the reflector curvature such that not all of these expressions are suited for diffractions. We introduce a new multiparameter traveltime expression, the implicit CRS (i-CRS) operator. It is suitable for media with arbitrary anisotropy. We demonstrate that it maintains its accuracy over the whole range of reflector curvatures, i.e., from nearly plane reflections to diffractions. Our investigations of the parameter estimation in VTI examples show that the geometry of the reflector as well as all pertinent elastic parameters, i.e., the vertical velocity as well as Thomsen's δ and ε can be determined with the i-CRS operator.

INTRODUCTION

Multiparameter stacking methods serve as important tools in applied seismics to obtain a reliable time image of the subsurface. Over the past years, several stacking operators have been introduced. They all aim to describe the traveltime moveout in both midpoint and offset direction for reflected and diffracted events with the highest possible accuracy. The three most prominent operators are the shifted hyperbola (de Bazelaire, 1988), the common reflection surface stack (CRS, Müller, 1999) and multifocusing (MF, Gelchinsky et al., 1999; Landa et al., 2010). Their accuracies in general differ and depend on the considered offset as well as on the reflector curvature. Furthermore, neither of these operators accounts for seismic anisotropy in the overburden.

Seismic anisotropy, however, is an important source for information. By inverting the observations one might obtain information going beyond the typical resolution of seismic waves, for instance about the composition of subsurface structures or the permeability tensor of rocks (e.g., Helbig and Thomsen, 2005). Therefore, the determination of the parameters characterising effects caused by seismic anisotropy is of outermost importance. This has been recognised and addressed in the context of developing long-spread nonhyperbolic moveout operators.

However, these operators usually assume that the nonhyperbolicity is caused by the underlying anisotropy. Furthermore, they do not allow to distinguish between effects from anisotropy and effects from heterogeneity. This is an inherent and so far unsolved issue when dealing with anisotropic media because both effects depend on the scale length of the problem. On the other hand, it is well known that nonhyperbolic moveout occurs already for horizontally stratified isotropic media at larger offsets (see, e.g.,

Tsvankin and Thomsen, 1994).

So far, anisotropic stacking operators have been limited to CMP stacking, i.e., stacking over offsets, only. Furthermore, most existing formulae do not consider curved subsurface structures (Fomel and Grechka, 2001). Finally, they do not allow to retrieve all pertinent elastic parameters from surface observations alone. For example, application of one of the most prominent operators for weak VTI media suggested by Alkhalifah and Tsvankin (1995) leads only to two parameters, namely the normal moveout velocity ($V_{NMO} = \alpha\sqrt{1+2\delta}$ for horizontally-stratified VTI media) and the anellipticity parameter ($\eta = \frac{\varepsilon-\delta}{1+2\delta}$), not however to the vertical velocity α . Whereas knowledge of V_{NMO} and η is sufficient for time imaging, α is required for the transformation to depth (e.g., Tsvankin et al., 2010).

Vanelle et al. (2010) have recently introduced a new traveltime expression for curved structures in isotropic media, referred to as implicit common reflection surface (i-CRS) operator. Their model-based approach splits the raypath into the up- and down-going ray from a circular interface. The actual reflection point is then gained by evaluating Fermat's principle, which yields implicit expressions for the traveltime surfaces. Because of its implicit character the operator can be applied recursively. Regarding the accuracy, the operator is superior for larger offsets and midpoint displacements and its results are independent of the reflector curvature.

In this work, we extend the approach by Vanelle et al. (2010) to account for anisotropy. After deriving the anisotropic i-CRS operator, we demonstrate its applicability with several examples. Comparison of i-CRS traveltimes with ray traveltimes confirms its accuracy. In subsequent experiments, we have investigated its sensitivity with regards to parameter determination. We find that for our VTI examples on *q*P-waves not only the anisotropy parameters α , δ , and ε can be determined, but also the reflector geometry. The section on our results is followed by a discussion and, finally, our conclusion that the new operator is a worthwhile extension of previous work.

METHOD

Note: for simplicity, we present the derivation for the 2D situation here. The extension to three dimensions is tedious but does not provide further insight to the problem.

We consider a circular reflector in a homogeneous medium. The radius of the reflector is R . Its centre is at the location (x_c, H) , as shown in Figure Ia. The coordinates x_1 and x_2 are those of a source and a receiver, respectively, both at the depth $z=0$. The angle θ defines the reflection point at $\mathbf{r} = (x_c + R \sin \theta, H - R \cos \theta)$. The ray/group velocities of the down- and up-going ray segments are $v_i(\vartheta_i)$ with the group velocity angles ϑ_i (see Figure Ib).

The traveltimes t_i of the down and up-going ray segments are given by

$$t_i^2 = \frac{(x_i - x_c - R \sin \theta)^2 + (H - R \cos \theta)^2}{v_i^2(\vartheta_i)}, \quad (1)$$

or, in midpoint and half-offset coordinates (x_m, h) :

$$t_1^2 = \frac{(x_m - h - x_c - R \sin \theta)^2 + (H - R \cos \theta)^2}{v_1^2(\vartheta_1)},$$

$$t_2^2 = \frac{(x_m + h - x_c - R \sin \theta)^2 + (H - R \cos \theta)^2}{v_2^2(\vartheta_2)}.$$

The traveltime of the reflected ray is

$$t = t_1 + t_2.$$

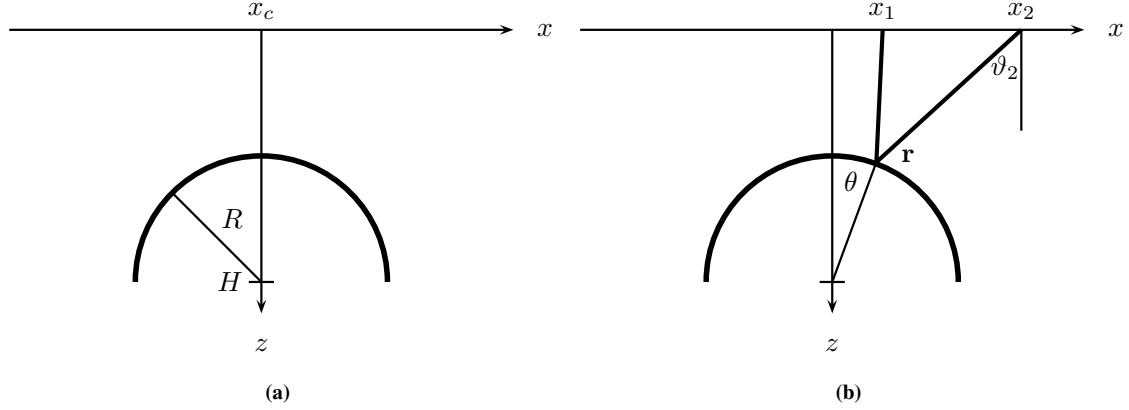


Figure 1: Geometry (a) and notations (b) for the circular reflector. The reflection point r is defined by the angle θ . The angles ϑ_i (only ϑ_2 is shown here) are the ray/group velocity angles.

The reflection traveltime t must fulfil Snell's law, i.e., $\partial t / \partial \theta = 0$. The derivatives of t_1 and t_2 with respect to θ are

$$\frac{\partial t_i}{\partial \theta} = \frac{1}{2 t_i} \frac{\partial t_i^2}{\partial \theta} = \frac{R}{v_i^2 t_i} [H \sin \theta - (x_i - x_c) \cos \theta] - \frac{t_i}{v_i} \frac{\partial v_i}{\partial \theta} \quad ,$$

where

$$\frac{\partial v_i}{\partial \theta} = \frac{\partial v_i}{\partial \vartheta_i} \frac{\partial \vartheta_i}{\partial \theta} \quad .$$

From the geometry of the ray paths shown in Figure 1b we have that

$$\tan \vartheta_i = \frac{x_i - x_c - R \sin \theta}{H - R \cos \theta} \quad ,$$

which leads us to

$$\frac{\partial \vartheta_i}{\partial \theta} = \frac{R}{v_i^2 t_i^2} (R - H \cos \theta - (x_i - x_c) \sin \theta) \quad ,$$

and finally to

$$\begin{aligned} \frac{\partial t}{\partial \theta} = & \underbrace{\left[\frac{H}{v_1^2 t_1} + \frac{H}{v_2^2 t_2} + \frac{x_1 - x_c}{v_1^3 t_1} \frac{\partial v_1}{\partial \vartheta_1} + \frac{x_2 - x_c}{v_2^3 t_2} \frac{\partial v_2}{\partial \vartheta_2} \right]}_A R \sin \theta \\ & + \underbrace{\left[\frac{H}{v_1^3 t_1} \frac{\partial v_1}{\partial \vartheta_1} + \frac{H}{v_2^3 t_2} \frac{\partial v_2}{\partial \vartheta_2} - \frac{x_1 - x_c}{v_1^2 t_1} - \frac{x_2 - x_c}{v_2^2 t_2} \right]}_B R \cos \theta \\ & + \underbrace{\left[-\frac{R}{v_1^3 t_1} \frac{\partial v_1}{\partial \vartheta_1} - \frac{R}{v_2^3 t_2} \frac{\partial v_2}{\partial \vartheta_2} \right]}_C R \quad . \end{aligned}$$

Introducing the abbreviations A , B , and C , as shown above, this equation can be shortened to

$$A \sin \theta + B \cos \theta + C = 0 \quad .$$

Its solution is

$$\sin \theta = -\frac{AC}{A^2 + B^2} \pm \frac{B}{A^2 + B^2} \sqrt{A^2 + B^2 - C^2} \quad , \quad (2)$$

where the negative sign must be chosen, as we can deduce from the isotropic case: if the velocities do not depend on direction, the expressions for the quantities A and B simplify considerably. Furthermore, C vanishes, and we find that

$$\tan \theta = -\frac{B}{A} .$$

The sign of $\sin \theta$ is negative because the cosine is positive for a reflection from the circle, i.e.,

$$\sin \theta = -\frac{B}{\sqrt{A^2 + B^2}} .$$

On the other hand, equation 2 collapses to

$$\sin \theta = \pm \frac{B}{\sqrt{A^2 + B^2}} .$$

Comparing the coefficients of these expressions lets us recognise that the negative sign must be chosen in equation 2.

Note that until here, all expressions are exact. Furthermore, they are equally applicable to converted waves in isotropic as well as anisotropic media. Since the group angles ϑ_i and thus the group velocities v_i and traveltimes t_i implicitly depend on θ , equation 2 cannot be directly solved for θ , though. We can, however, apply equation 2 in a recursive fashion where we choose an initial zero-offset angle θ_0 to obtain an update for θ from equation 2, which can then be used to compute the traveltimes t_i with equation 1. Further iterations can be applied to enhance the accuracy.

In the 3D case, we have to consider eight parameters, namely two radii of curvature and the six x , y , and z coordinates of the respective centres, instead of the three parameters for the reflection from the circle in 2D (two coordinates for the centre of the circle and its radius). The extension to heterogeneous media will be addressed below in the Discussion section, after we demonstrate different applications of the operator in the next section.

RESULTS

This section begins with an investigation of the new anisotropic i-CRS operator regarding traveltime errors. For the applicability of the operator to the estimation of anisotropy and geometry parameters, we have then carried out a feasibility study. We show results from this study where we have analysed the sensitivity of the parameter determination. The section concludes with examples for the parameter estimation.

Traveltimes

We begin with the verification of the accuracy of the i-CRS operator. This has to be carried out in two steps: although the expressions are exact, they cannot be applied directly, as already mentioned above. In conclusion, we must evaluate the introduction of errors through the iterative approach and the operator's implicit nature.

On the other hand, the operator requires that expressions are available for the group velocities in terms of the group angles. Such expressions do not generally exist because computations are usually based on phase angles rather than group. Existing formulations assume that the anisotropy is weak (see, e.g., Thomsen, 1986). This assumption, however, also introduces errors that have to be investigated as well as separated from the errors due to the iteration process.

In order to evaluate both error contributions individually, we have chosen a medium with elliptical symmetry, where Thomsen's parameters $\varepsilon = \delta$ coincide. Only in this case is it possible to find a closed-form exact expression for the group velocity in terms of the group angle.

For our investigation, we have generated reference traveltimes with the NORSAR ray modelling software for q P-waves for the following reflector geometry, anisotropy parameters, and acquisition:

- the lateral coordinate of the centre of the circle was located at $x_c=0$,
- three circle radii were considered, namely $R=100$ m, 1000 m, and 10 000 m,
- the depth of the top of the reflector, $H - R$, was 1000 m,
- the acquisition comprised midpoints between 0 and 1000 m and offsets up to 2000 m,
- the vertical velocity was $\alpha=4000$ m/s,
- Thomsen's parameters $\varepsilon = \delta$ were varied from 0 (the isotropic case) to 0.4, which signifies rather strong anisotropy.

The i-CRS operator was then applied twice to each data set and the results were compared to the reference traveltimes. In the first experiment, we used the exact expressions for the group velocity and its derivative,

$$v_i = \frac{\alpha}{\sqrt{\frac{\sin^2 \vartheta_i}{1+2\varepsilon} + \cos^2 \vartheta_i}} \quad ,$$

$$\frac{\partial v_i}{\partial \vartheta_i} = \frac{2 v_i^3 \varepsilon}{\alpha^2 (1 + 2\varepsilon)} \sin \vartheta_i \cos \vartheta_i \quad .$$

In the second experiment, we applied the weak anisotropy approximation given by Thomsen (1986),

$$v_i = \alpha (1 + \delta \sin^2 \vartheta_i + (\varepsilon - \delta) \sin^4 \vartheta_i) \quad ,$$

$$\frac{\partial v_i}{\partial \vartheta_i} = 2 \alpha \sin \vartheta_i \cos \vartheta_i (\delta + 2 (\varepsilon - \delta) \sin^2 \vartheta_i) \quad .$$

The resulting RMS errors are presented in Figure 2. We find high accuracy for all reflector radii if exact expressions for the velocities and derivatives are available. This means that the i-CRS operator itself performs with high precision. If the velocities and derivatives are substituted by their weakly anisotropic counterparts, the accuracy degrades with increasing strength of anisotropy, which agrees with our expectations.

After establishing the accuracy of the i-CRS operator, we have investigated its application to the estimation of anisotropy parameters and geometric properties of the model. The first step was a feasibility analysis, which considers the sensitivity of the parameter estimation. The results are presented in the following section.

Sensitivity analysis

A first sensitivity analysis for parameter estimation was recently introduced by Tygel et al. (2011) for the nonhyperbolic CRS operator (Fomel and Kazinnik, 2012). The basic idea of their strategy is that, if the traveltimes does not respond to perturbations of a certain parameter, this parameter cannot be estimated accurately. If, on the other hand, the traveltimes varies much, the objective function for the parameter estimation has a more pronounced extremum for the correct value. In this section, we carry out a corresponding sensitivity analysis for the parameters of the i-CRS operator.

We have chosen a medium with weak VTI anisotropy for this investigation, Mesaverde Shale (350) from Thomsen (1986). The anisotropy parameters of this medium are summarised in Table 1. The geometry and acquisition were chosen as follows:

- the lateral coordinate of the centre of the circle was located at $x_c=-500$ m,
- the radius of the circle was $R=1000$ m,
- the depth of the top of the reflector, $H - R$, was at 1000 m,

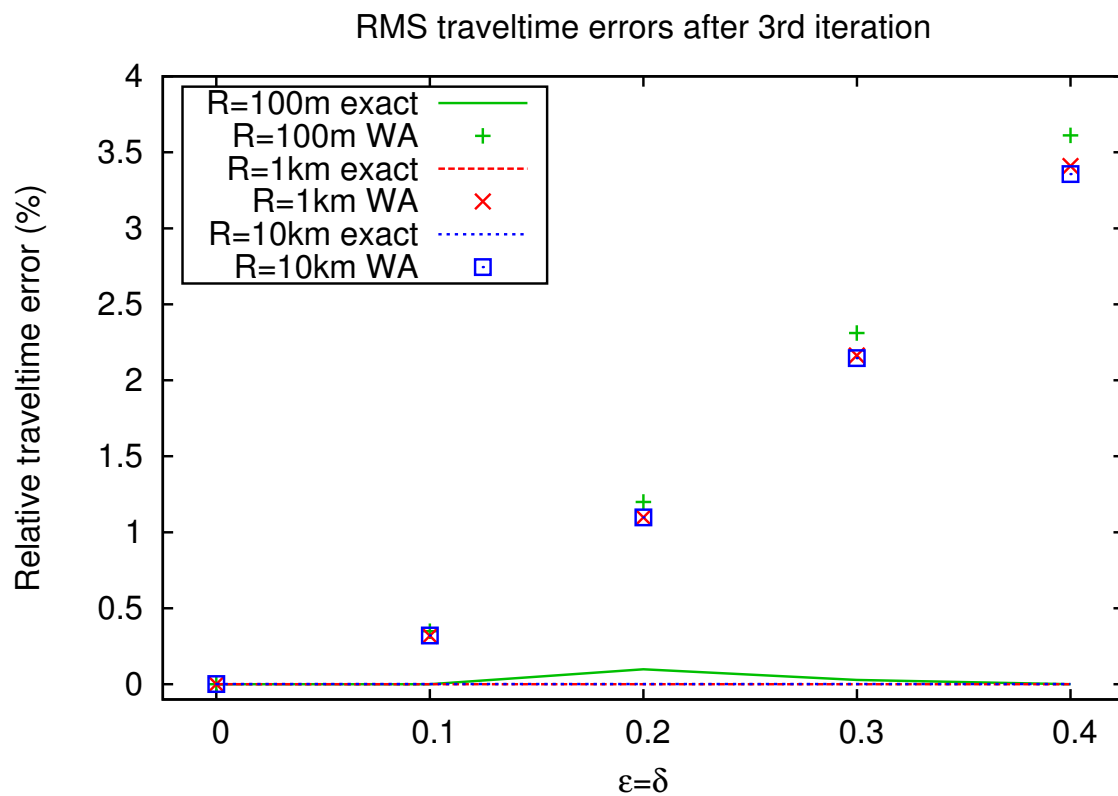


Figure 2: Accuracy of the i-CRS stacking operator after three iterations in the presence of elliptical anisotropy. Lines indicate that the new operator performs with high accuracy for all reflector radii if exact velocities and derivatives are used. If these are expressed by their weakly anisotropic (denoted WA) counterpart, the accuracy degrades with increasing strength of anisotropy. Note that the slightly higher errors for the smallest (100 m) radius are introduced by errors in the reference traveltimes.

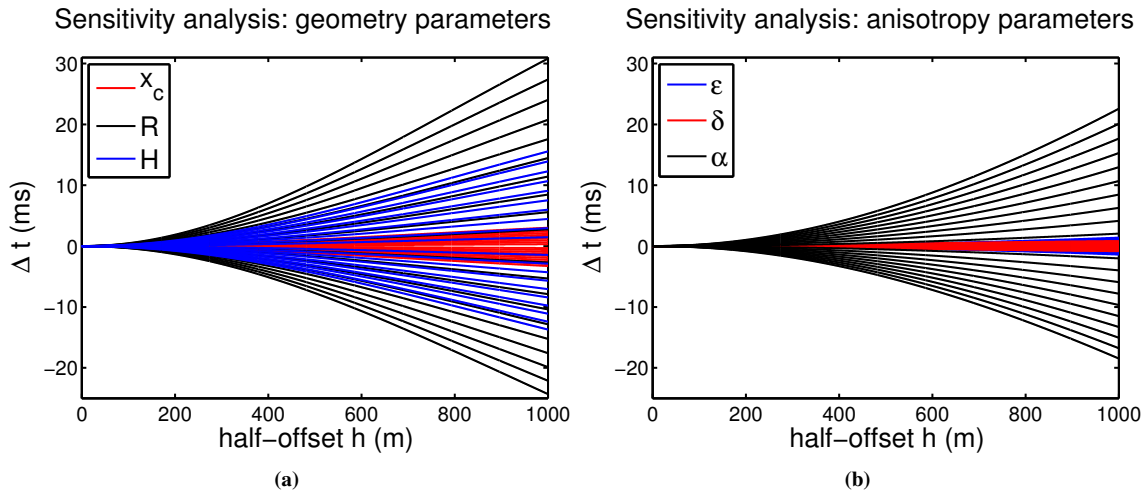


Figure 3: Sensitivity of the i-CRS traveltimes with respect to the parameters for the weakly anisotropic medium 1. (a) Sensitivity of the geometry parameters if they are perturbed within a range of $\pm 10\%$ of their original values in steps of 1%. (b) Sensitivity of the anisotropy parameters if they are perturbed within a range of $\pm 10\%$ of their original values. Large traveltimes deviations correspond to a high sensitivity for the respective parameter.

- the acquisition comprised offsets up to 2 km,
- the CMP position was located at $x_m=0$ m.

While varying one parameter from -10% to $+10\%$ of its correct value in steps of 1%, the correct values were assigned to the other parameters. Figure 3 displays the resulting traveltimes deviations.

Figure 3a presents the traveltimes deviations Δt that result from the perturbations of the geometry parameters x_c , R and H in reference to the traveltimes following from the correct parameters. In comparison to R and H , the variation of the lateral position x_c results in smaller traveltimes deviations. We therefore expect a lower sensitivity for this parameter. Figure 3b shows that the sensitivity of the vertical P-wave velocity α is similar to that of R and H . The effects of perturbing Thomsen's parameters ϵ and δ , however, are relatively small, meaning that their values are expected to be less accurate than those of R , H , and α .

In the next section, we demonstrate the parameter estimation with examples.

Parameter estimation

In this section we investigate if our new operator is capable of detecting anisotropy, and, if so, quantifying it, and possibly separating the effects from lateral heterogeneity, i.e., curved structures. For this purpose, we have generated traveltimes with the NORSAR ray modelling software for a circular reflector in two different homogeneous VTI media. The survey design and parameters were as follows:

- the lateral coordinate of the centre of the circle was located at $x_c=-500$ m,
- the radius of the circle was $R=1000$ m,
- the depth of the top of the reflector, $H - R$, was at 1000 m,
- the acquisition comprised midpoints between 0 and 1000 m and offsets up to 2000 m,
- the parameters for the two VTI media are given in Table 1, where medium 1, Mesaverde Shale, is weakly anisotropic, while medium 2, Shale 5000, exhibits stronger anisotropy (Thomsen, 1986).

Table 1: Relevant elastic parameters and relative RMS traveltimes errors for the VTI media Mesaverde Shale (350) and Shale (5000) after Thomsen (1986).

	Name	α (m/s)	ε	δ	Δt_{RMS}
Medium 1	Mesaverde Shale (350)	3383	0.065	0.059	0.123 %
Medium 2	Shale (5000)	3048	0.255	-0.05	0.880 %

For each of these media, we have conducted three different experiments:

- the geometry parameters were determined while the anisotropy parameters were prescribed to their exact values,
- the anisotropy parameters were determined while the geometry parameters were prescribed to their exact values,
- all parameters were determined simultaneously.

The parameter search was carried out by a Nelder-Mead optimisation scheme (Nelder and Mead, 1965). In order to illustrate the accuracy of the resulting parameters, we display the reflector geometry for the exact and determined parameters in Figure 4a for the weakly anisotropic medium 1 and in Figure 5a for the strongly anisotropic medium 2. We observe that the simultaneous search for all parameters, i.e., anisotropy as well as geometry parameters, leads to a better match than the search for only the geometry parameters if the anisotropy parameters are prescribed as their exact values. The deviation is particularly visible for the medium with the stronger anisotropy. This result is, however, not surprising because the weak anisotropy approximation reduces the accuracy if the anisotropy is strong.

Similarly, Figures 4b and 5b show wavefronts resulting from the searches for all parameters simultaneously, and the anisotropy parameters for prescribed correct geometry. These wavefronts were computed with the weak anisotropy approximation because the parameter determination is based on it. The wavefronts denoted 'exact' for comparison use the correct parameters and the exact group velocity expression since these wavefronts correspond to the input traveltimes. Here, we observe that the determination of only α , δ , and ε leads to better results. Again, the match between exact and determined parameters is better for the weakly anisotropic medium.

In addition, we have plotted the relative errors of the parameter estimation for both media and all experiments in Figure 6. This figure shows that the estimation of the geometry is overall more accurate than that of the anisotropy. As we expect from the sensitivity analysis, the vertical velocity α can be better determined than δ and ε . Despite deviations of up to 30 % for medium 1, the wavefront in Figure 4b is still very close to the exact one. The large error in δ for medium 2 in the case of the simultaneous search for all parameters leads to the high deviation of the wavefront in Figure 5b. However, as we have already pointed out, this is a result of the weak anisotropy approximation, which is not valid for medium 2.

Since the geometry is determined best from a simultaneous search for all parameters while the anisotropy parameters fit better if the geometry is prescribed, it may be suggested to apply a two-step procedure as follows: in the first step, a simultaneous search for all parameters is carried out. The geometry parameters obtained with this step would then be used as input for the anisotropy parameter search. However, the anisotropy parameters determined in this second step are the exact same values we obtain from the simultaneous search for all parameters as these already minimise the objective function for this geometry.

In a final test, we have verified that the i-CRS operator can be used for the detection of seismic anisotropy by applying it to isotropic data. Again, the geometry was chosen as $x_c = -500$ m, $H = 2000$ m,

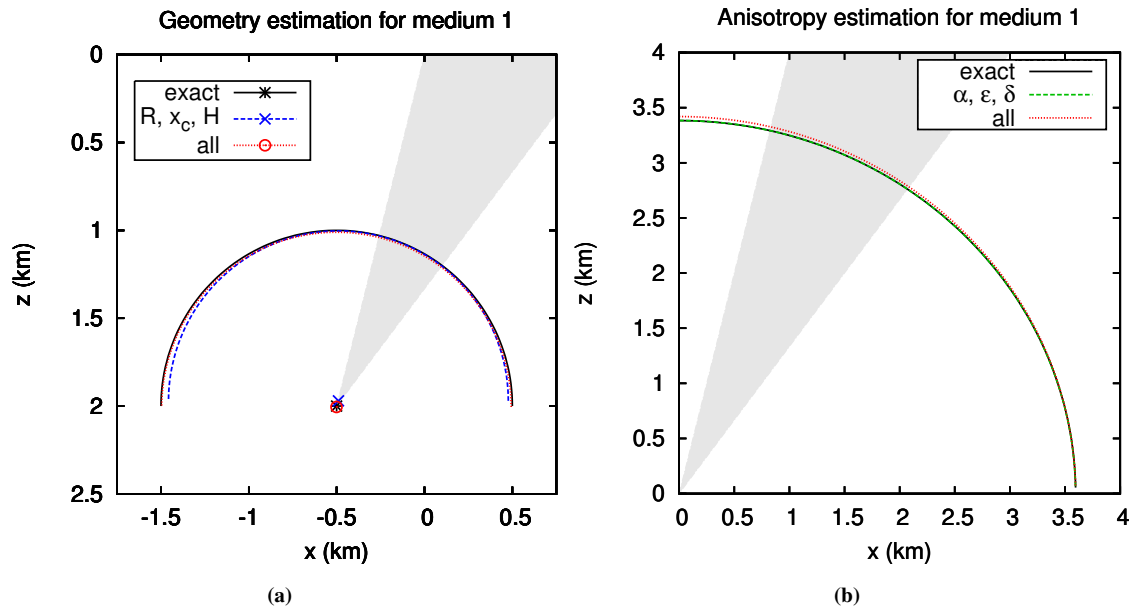


Figure 4: Accuracy of the parameter determination for medium 1, which exhibits weak anisotropy. (a) Reconstructed geometry (denoted by lines for the circle and symbols for its centre) if the exact values (black), values from a search with prescribed correct anisotropy parameters (blue), and values from a simultaneous search for all parameters (red) were used. (b) Reconstructed wavefronts for $t=1$ s if the exact values (black), values from a search with prescribed correct geometry parameters (green), and values from a simultaneous search for all parameters (red) were used. The grey-shaded area outlines the illumination, the ray coverage provided by the acquisition.

and $R=1000$ m, and the constant velocity was 4000 m/s. For the starting values, these quantities were perturbed by 20 %, and the anisotropy parameters were initialised to $\delta=0.1$ and $\epsilon=0.1$. The geometry was reconstructed with maximum errors below 8 cm. The velocity resulted in $v=3999.72$ m/s, and the values for δ and ϵ were both obtained as 0.0001, i.e., practically zero, despite their initialisation with a much higher value.

This final test confirms that the i-CRS operator can indeed be applied for the detection of anisotropy, where the previous experiments already showed that existing anisotropy can be quantified.

DISCUSSION

The results of the traveltimes investigation show that the operator is not only well-suited for the description of reflections but also for diffraction events, i.e., small radii of curvature. For homogeneous isotropic media, we found in addition that the i-CRS's accuracy is higher than that of other multiparameter stacking techniques like multifocusing or CRS (Vanelle et al., 2010).

In isotropic media, the i-CRS operator has been extended to heterogeneity (Schwarz, 2011). Application to the complex synthetic Sigsbee 2A data set shows that i-CRS yields superior results compared to CRS, especially in regions with small scale structures and diffractors like the rugged top of salt (Schwarz, 2011).

The i-CRS operator can be applied to anisotropic heterogeneous media as it is. In this case, the parameters become effective parameters, which no longer have a clear physical meaning. Such parameters have been widely accepted in anisotropic NMO/DMO stacking (e.g., Wang and Tsvankin, 2009). However, with current anisotropic stacking methods, according to Tsvankin et al. (2010) the parameters α , δ , and

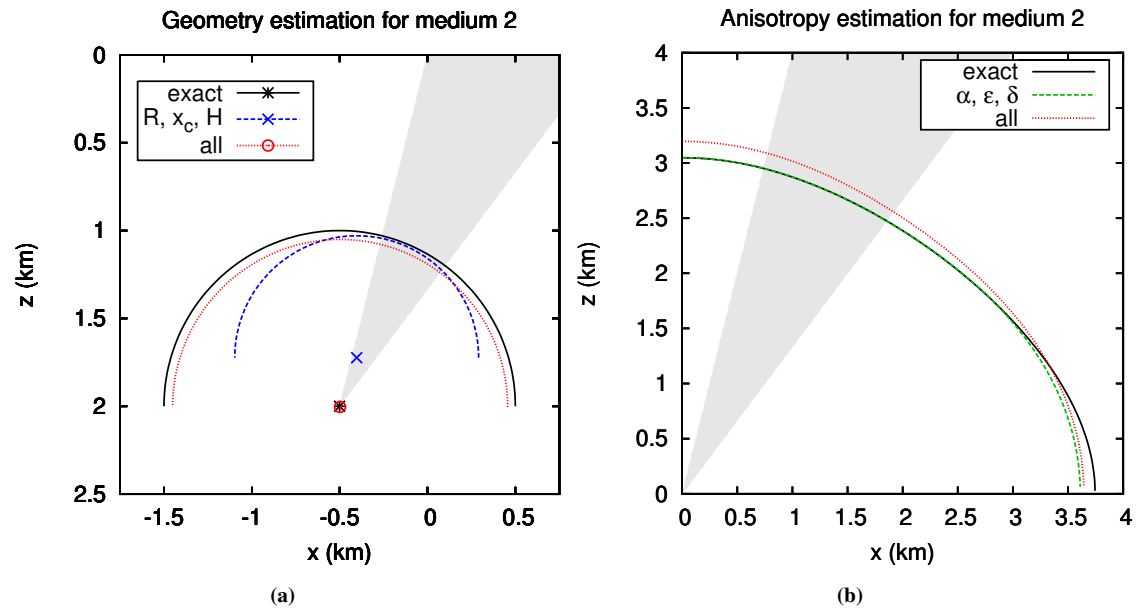


Figure 5: Accuracy of the parameter determination for medium 2, which exhibits strong anisotropy. (a) Reconstructed geometry (denoted by lines for the circle and symbols for its centre) if the exact values (black), values from a search with prescribed correct anisotropy parameters (blue), and values from a simultaneous search for all parameters (red) were used. (b) Reconstructed wavefronts for $t=1$ s if the exact values (black), values from a search with prescribed correct geometry parameters (green), and values from a simultaneous search for all parameters (red) were used. The grey-shaded area outlines the illumination, the ray coverage provided by the acquisition.

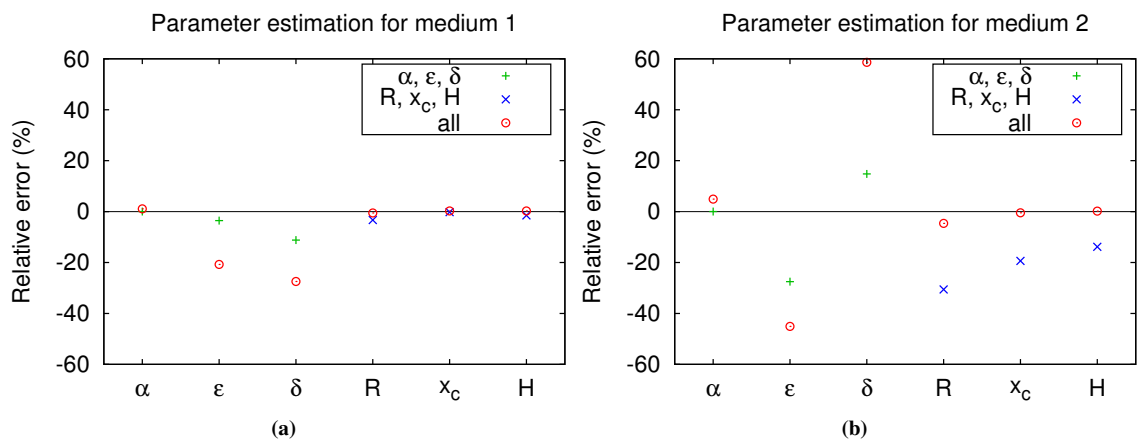


Figure 6: Relative errors of the parameter estimation (a) for the weakly anisotropic medium 1, and (b) for the strongly anisotropic medium 2. The black solid line corresponds to zero. Red circles show percentage errors if all parameters were optimised simultaneously. Blue crosses indicate the errors of the geometry determination if the exact anisotropy parameters were prescribed. Green plus symbols indicate the errors of the anisotropy determination if the exact geometry parameters were prescribed.

ε can seldomly be determined from P-wave moveout alone. The i-CRS operator can provide all three parameters from surface measurements.

The physical interpretation of the effective parameters in anisotropic media is more complex than in the isotropic case. For the latter, Schwarz (2011) has succeeded in relating the model-based i-CRS parameters to the surface-based CRS parameters (Müller, 1999). These correspond to the emergence/incidence angles and curvatures of wavefronts in the registration surface. Since a corresponding CRS description does not exist for anisotropic media, this problem is still an unsolved challenge, which we are currently investigating.

The operator is also applicable to converted waves. As the conversion point dispersal is, however, larger than the reflection point dispersal for monotypic waves, a representation in midpoint and half-offset coordinates is no longer feasible. Converted wave data are, therefore, usually stacked in common-conversion-point (CCP) rather than CMP gathers (e.g. Tessmer and Behle, 1988, 1990). Since the CCP stacking does not consider the curvature of interfaces, Abakumov et al. (2012) have recently introduced the so-called γ -CMP coordinates, which allow for stacking in the presence of curved reflectors. These coordinates should also be adopted for the application of the i-CRS technique.

It may be argued that since the i-CRS operator has more parameters, i.e., the geometry in addition to the anisotropy parameters, it will in any event provide a better fit to the traveltimes than other established operators. We conclude from our examples that the i-CRS provides a better fit because it is physically sound, and not because it has more parameters. This conclusion is supported in particular by our final example where the anisotropy parameters δ and ε were returned as zero for an isotropic medium. If the good fit were indeed due to the number of parameters, these values would not be equal to zero.

If the anisotropy is weak, the i-CRS operator leads to convincing results for the traveltimes approximation as well as for the determination of parameters. A current weakness lies in the applicability to media with strong anisotropy. Although the i-CRS method itself does not underlie any restrictions regarding the model, we have so far used a weak anisotropy approximation to express the group velocities and their derivatives. In order to include strong anisotropy, new expressions for the group velocity in terms of group angles need to be developed. One possibility is a representation of the group velocity that was recently published by Dell et al. (2012).

CONCLUSIONS

With the anisotropic i-CRS operator, we have introduced a new multiparameter traveltimes expression. The operator is derived for a locally curved interface and applicable to media with arbitrary anisotropy. The strength of curvature of the reflector under consideration does not influence the accuracy of the operator, which makes it suited for diffractions as well as for reflections.

In addition to an accurate description of the traveltimes, the operator yields the subsurface geometry and all pertinent anisotropy parameters, thus allowing to distinguish between effects introduced by anisotropy and structural heterogeneity. For the VTI models we have investigated, we obtained not only Thomsen's δ and ε from surface observations, but also the vertical P-wave velocity α . With other techniques, only two parameters, usually the normal moveout velocity V_{NMO} and the parameter η , are available from surface observations. Therefore, the i-CRS operator provides an important extension of previous work.

If heterogeneities are present, all parameters become effective ones and lose their physical meaning in relation to the real subsurface model. In this case, the effective geometric parameters describe a reflector in a corresponding homogeneous medium defined by the effective anisotropy parameters. We are at present working on an extension to heterogeneity that allows a physical interpretation of the effective parameters, e.g., in terms of wavefront curvatures measured in the registration surface.

Although the i-CRS is valid for arbitrary anisotropy, the current implementation makes use of a weak

anisotropy approximation in order to express group velocities in terms of group angles. Accordingly, the accuracy of the operator in this implementation degrades in the presence of strong anisotropy. In order to overcome this limitation, we are currently investigating alternative expressions for the group velocities.

ACKNOWLEDGEMENTS

The authors thank Martina Bobsin for providing the anisotropic traveltimes, which were generated with the NORSAR Seismic Modelling Software. We are grateful to Alexander Bauer and the members of the Applied Seismics Group in Hamburg for continuous discussion. This work was partially supported by the sponsors of the Wave Inversion Technology (WIT) consortium and the project 'Imaging steep structures with diffractions' (BMU 0325363C).

REFERENCES

- Abakumov, I., Kashtan, B., Schwarz, B., Vanelle, C., and Gajewski, D. (2012). Double-square root travel-time approximation for converted waves. In *SEG 82nd Annual Meeting, Expanded Abstracts*.
- Alkhalifah, T. and Tsvankin, I. (1995). Velocity analysis for transversely isotropic media. *Geophysics*, 60:1550–1566.
- de Bazelaire, E. (1988). Normal moveout revisited – inhomogeneous media and curved interfaces. *Geophysics*, 53:143–157.
- Dell, S., Gajewski, D., and Kashtan, B. (2012). Diffraction traveltime approximation for an arbitrary anisotropic medium. In *15th International Workshop on Seismic Anisotropy, Expanded Abstracts*.
- Fomel, S. and Grechka, V. (2001). Nonhyperbolic reflection moveout of P-waves. An overview and comparison of reasons. Technical Report CWP-372, Colorado School of Mines.
- Fomel, S. and Kazinnik, R. (2012). Non-hyperbolic common reflection surface. *Geophysical Prospecting*, pages doi: 10.1111/j.1365–2478.2012.01055.x.
- Gelchinsky, B., Berkovitch, A., and Keydar, S. (1999). Multifocusing homeomorphic imaging – Part 1. Basic concepts and formulae. *Journal of Applied Geophysics*, 42:229–242.
- Helbig, K. and Thomsen, L. (2005). 75-plus years of anisotropy in exploration and reservoir seismics: A historical review of concepts and methods. *Geophysics*, 70:9ND–23ND.
- Landa, E., Keydar, S., and Moser, T. J. (2010). Multifocusing revisited – inhomogeneous media and curved interfaces. *Geophysical Prospecting*, 58:925–938; doi: 10.1111/j.1365–2478.2010.00865.x.
- Müller, T. (1999). *The Common Reflection Surface stack method – seismic imaging without explicit knowledge of the velocity model*. PhD thesis, University of Karlsruhe.
- Nelder, J. and Mead, R. (1965). A simplex method for function minimization. *American Mathematical Monthly*, 105:523–528.
- Schwarz, B. (2011). A new nonhyperbolic multi-parameter stacking operator. Master's thesis, University of Hamburg.
- Tessmer, G. and Behle, A. (1988). Common reflection point data stacking technique for converted waves. *Geophysical Prospecting*, 36:671–688.
- Tessmer, G. and Behle, A. (1990). Conversion points and traveltimes of converted waves in parallel dipping layers. *Geophysical Prospecting*, 38:387–405.
- Thomsen, L. (1986). Weak elastic anisotropy. *Geophysics*, 51:1954–1966.

- Tsvankin, I., Gaiser, J., Grechka, V., van der Baan, M., and Thomsen, L. (2010). Seismic anisotropy in exploration and reservoir characterization: an overview. *Geophysics*, 75:A15–A29.
- Tsvankin, I. and Thomsen, L. (1994). Nonhyperbolic reflection moveout in anisotropic media. *Geophysics*, 59:1290–1304.
- Tygel, M., Perroud, H., Lopes, R., and Krummenauer, R. (2011). Sensitivity analysis of the non-hyperbolic Common Reflection Surface. *15th Annual WIT Report*, pages 333–342.
- Vanelle, C., Kashtan, B., Dell, S., and Gajewski, D. (2010). A new stacking operator for curved subsurface structures. In *SEG 80th Annual Meeting, Expanded Abstracts*.
- Wang, X. and Tsvankin, I. (2009). Estimation of interval anisotropy parameters using velocity-independent layer stripping. *Geophysics*, 74:WB117–WB127.